2022 Building Performance Modeling Conference and
SimBuild co-organized by ASHRAE and IBPSA-USA
Chicago, IL
September 14-16, 2022

Optimal Sizing of Integrated Community Energy Systems Considering Equity Constraints

Christoph Gehbauer[1], Yulun Wu[2], James Brown[1 2], and Michael Sohn[1]
[1]Lawrence Berkeley National Laboratory, Berkeley, CA
[2]University of California Berkeley, Berkeley, CA

Abstract

Integrated energy systems (IES) describe a holistic approach to finding coordinated energy and economic solutions. IES have the potential to mitigate inequities which can arise from grid, space, or economic limitations. This paper introduces a simulation environment to model IES and provides a parametric analysis of battery sizes through an optimal control strategy to assess the potential of IES. The electricity cost savings for controls integration through IES ranged up to 10.0 % on an annual basis and up to 23.5 % for certain periods. Equitable and economic access to green energy can be provided by sharing resources through IES.

Introduction

Integrated Energy Systems (IES) broadly describes a holistic approach to finding coordinated energy and economic solutions from across a wide range of energy options. These energy systems can include (a) production, e.g., solar, wind, hydro, biofuels, (b) conveyance, e.g., electricity, thermal, hydrogen, (c) storage, e.g., daily, seasonal, and (d) customer-level use, e.g., buildings, transportation, industry. At present, these systems are linked, but they typically function separately or respond individually depending on a wide range of disparate system-operation goals. The inability to link these systems may limit the ability to find economically favourable zero-carbon energy solutions across sectors (Shandiz, Rismanchi, and Foliente 2021).

Particularly the interactions between buildings and the electric power grid are becoming increasingly complex with the transition to a decarbonized future. Buildings, as the largest consumer of electricity, pose the potential to actively control demand and trade energy across sites, facilitating this transition by matching demand to generation from intermittent renewable generation (Neukomm, Nubbe, and Fares 2019). The integration of multiple building sites and technologies through IES pose potential benefits of carbon emission, cost, and inequitatble energy reductions (Bakhtavar et al. 2020) and (Vezzoli et al. 2018). Planning and operating an IES without considering the social equity could result in inequitable access to clean energy (Baker, Goldstein, and Azevedo 2021). However, interrogating such systems is non-trivial, and requires timestep-to-timestep interactions across multi-domain simulators which are hard to solve (Mendes, Ioakimidis, and Ferrão 2011). This effect is especially apparent when equity is considered where potentially large differences in available resources exist, making individual control without knowledge of other sites inefficient. Inequities can arise from (a) grid limitations, e.g., power flow or voltage constraints, (b) space limitations, e.g., high and narrow buildings have less roof space for photovoltaics, or (c) economic factors, e.g., disadvantaged communities. On the other hand, including knowledge of inequity allows the adjustment of adjacent resources which may result in greater benefit for the whole community.

In this paper we introduce our latest development of a simulation environment containing IES to explore the potential of economic, reliability, and operational interactions. The environment is demonstrated through parametric optimal sizing of distributed battery storage for an IES. In particular, the building-to-building and building-to-grid interactions are interrogated to resolve inequities in access of economic carbon-reducing technologies. The goal of this study is to estimate the technical potential of IES. With the development of this platform, we hope to consider how and what equity means for energy integration and how to simulate such concerns.

Methodology

An expandable simulation environment was developed using mostly publicly available simulation models and coupled through the Functional Mock-up Interface (FMI) (Modelica 2022), an industry standard for coupling of simulation models. The simulation is built in a modular fashion using the FMI which allows the export and coupling of third-party simulators. This bears the advantage that existing, specialized simulation tools can be leveraged to form a high-fidelity IES simulation environ-

ment. For instance, detailed building simulation models can be exported from EnergyPlus, electric vehicle models from Modelica, and control models from Matlab, and all coupled through the FMI development. To date, the FMI supports over 150 simulation tools where simulation models can be exported or imported. The developed simulation environment utilizes the Functional Mock-up Interface - Machine Learning Center (FMI-MLC) as a high-level wrapper of FMI to couple and parameterize the individual simulators (Gehbauer, Rippl, and Lee 2021). The multiple simulators are tightly coupled and require timestep-to-timestep interactions to exchange current inputs and states with each other. A custom simulation orchestrator was developed to couple the individual simulators and integrated with the FMI-MLC. This custom orchestrator was necessary to allow multi-timestep interactions where simulation models communicated with each other on a five minute timestep to handle transitory dynamics, while external communication with the controller was set to an hourly timestep.

The developed simulation environment consists of detailed building physics models, distributed energy resources, and predictive control system. For this study a derivate of the IEEE13 prototypical test feeder was used to represent the electrical distribution network for 13 electrical distribution nodes with 12 load-bearing nodes, representing up to 135 individual customer sites in this study. Each site includes either medium office or mid-rise apartment Department of Energy (DOE) reference buildings with co-located Photovoltaic (PV) generation and stationary battery storage. The PV systems are connected to the grid through state-of-the-art smart inverters providing active and reactive power control. Figure 1 illustrates the simulation environment.

The electric power grid, in orange, was inspired by the IEEE13 prototypical feeder with similar total loading and topology, but without transformers or switches. It was exported from the Smart Control of Distributed Energy Resources (SCooDER) package in Modelica (Gehbauer et al. 2020). Each of the sites, in green, include (a) EnergyPlus building physics model with either medium office or mid-rise apartment DOE prototypical building exported through the EnergyPlusToFMU tool (Nouidui, Lorenzetti, and Wetter 2013), (b) PV generation model exported from the Modelica Buildings Library (Wetter et al. 2014), (c) stationary behind-the-meter battery storage exported from SCooDER, and (d) smart inverter, with voltage-dependent active and reactive power actuation to moderate grid voltage at point of common coupling, exported from SCooDER. For a fully populated IEEE13 feeder this results in at least 49 individual simulators which are coupled through the FMI-MLC shown as the blue outline. The exchange variables are denoted in Figure 1. Most relevant for this study are individual site's battery setpoint, P_{set_batt} in W, thermostat setpoint, T_{set_in} in C, battery state of charge, SOC_{batt} in %, and building average temperature, T_{in} in C. The simulation environment allows the coupling of external controllers, red outline, though OpenAI's Gym wrapper (Brockman et al. 2016) which defines *action* as input vector, *state* as output vector, and *reward* as scalar objective. Utilizing this standardized interface for control allows the connection of most machine learning developments to rapidly explore the high-dimensional interdependencies of IES. Control actions were the battery setpoint and building thermostat setpoint for each of the 12 sites. States were the battery state of charge, building average temperature, and power flow of each site, as well as time of day and weather data for temperature and solar irradiation. In addition, 24 hour forecasts for weather, PV generation, and building internal loads, i.e., equipment and people, were passed to the controller through the states object. The reward was set to the time-of-use (TOU) electricity cost of the whole community, including grid losses. This study used Pacific Gas and Electric's E-19 tariff. It includes three pricing periods, (I) off-peak from 22:00 to 8:00, (II) mid-peak from 8:00 to

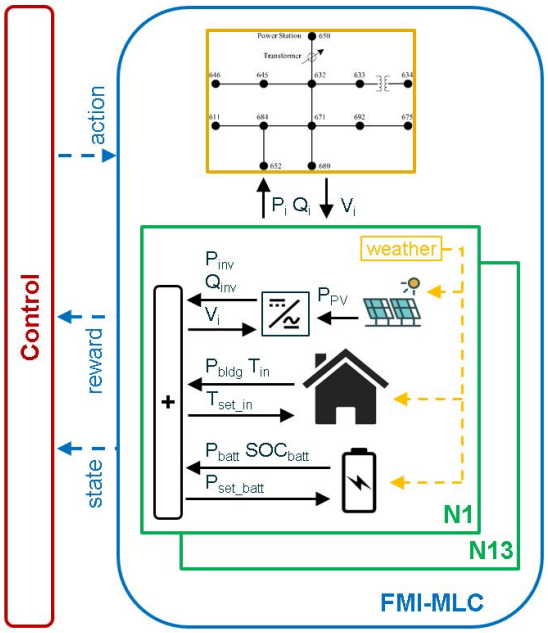

Figure 1: Overview of Simulation Environment with Simplified Information Flow.

12:00 and 18:00 to 22:00, and (III) on-peak from 12:00 to 18:00, in summer, May through October, and two periods, (I) off-peak from 22:00 to 8:00, and (II) mid-peak from 8:00 to 22:00, in winter. The cost periods for energy are 0.09496, 0.12656, and 0.17427 $/kWh in summer and 0.10280 and 0.12002 $/kWh in winter. The demand charges are 0, 6.10, and 21.10 $/kW in summer, and 0 and 0.14 $/kW in winter.

For this study, Model Predictive Control (MPC) was utilized to control each building's thermostat setpoint and battery power. Thermostat control setpoints were implemented in a fail-safe fashion, i.e., only changes within a range of setpoints were permitted, to restrict any occupant comfort violations. MPC was chosen because of its ability to provide optimality, when MPC-internal model matches the simulation model, and its raising interest in smart building control. In particular, an MPC system based on the Distributed Optimal and Predictive Energy Resources (DOPER) (Gehbauer et al. 2020) platform was utilized. The optimization horizon was set to 24 hours with hourly re-optimization to track optimal control setpoints. In order to evaluate the technical potential of IES, weather and load forecast uncertainty was set to zero. The model mismatch between the complex building simulation model and MPC-internal model was resolved by the introduction of a reduced-order resistor-capacitor (RC) model derived from EnergyPlus. Resulting root mean square errors for the RC model with June 1st as training day were 0.07 K for medium office and 0.005 K for mid-rise apartment. This reduced-order model was used for MPC and replaced EnergyPlus in the simulation environment which lead to a matched-model setup between simulation and control. Without forecast uncertainty and matched models between IES simulation environment and MPC, the only remaining mismatch was the lack of a grid model in the MPC. This shortcoming is only apparent during situations of high smart inverter actuation, e.g., when large amounts of reactive power are injected in the grid. The primary optimization objective was defined as TOU energy and demand cost with grid emissions as secondary objective. Control strategies included *individual*, i.e., each site optimizes for its local objective, and *integrated*, i.e., sites work together as a community and exchange energy, to assess the benefit of integration.

The base scenario chosen for this paper was derived using stochastic load and resource allocations to represent similar total loading as defined by the original IEEE13 network. Two scenarios of PV generation were explored: *peak* sizing which used a PV system sized to cover the daytime peak load during a sunny day in summer, and *net-zero* sizing which used a PV system sized to net-zero energy demand on a sunny day in summer. The climate was set to the DOE reference climate zone 3B-C which is a coastal climate in Los Angeles, CA. In order to evaluate optimal battery sizes, the Typical Meteorological Year (TMY) historic weather data was analyzed to identify most unique weather patterns. The k-means machine learning technique was applied to determine hyper cube clusters based on season, weekday or weekend, outdoor air temperature, and global horizontal irradiation. An optimal number of 16 clusters were identified and historic days closest to centroids were selected for the simulation study. Optimality was defined where incremental decline in error, i.e., sum of squared distances to centroids, converged towards a threshold of 0.5. Each cluster's weight was determined by the respective number of days and used to scale cluster results to annual projections. The number of days per cluster ranged from 12 to 44.

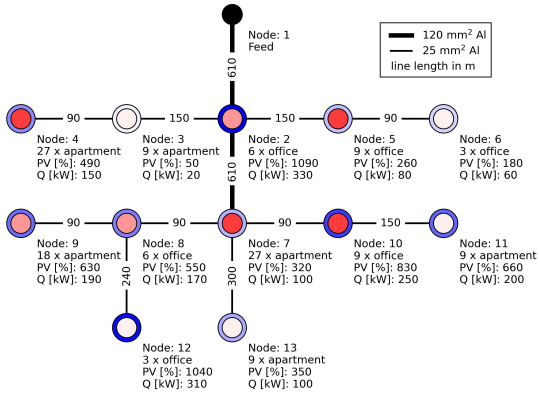

Figure 2: Electric Power Grid with Net-Zero PV Sizing Scenario.

Figure 2 illustrates the PV and loading allocations for the net-zero scenario. Node 1 represents the interconnection with the larger power grid feeding the radial distribution of customers. The inner color of each node represents its demand through multitude of office or apartment buildings. The darker the color, the higher its demand. PV size is indicated by the outer color. The scenario's load allocation represents 135 individual buildings across the 13 nodes, with 36 medium office buildings and 99 mid-rise apartments. Buildings were aggregated per node, which resulted one unique building simulation model per node. It can be seen that nodes 4, 5, 7, and 10 were most heavily loaded with up to nine medium office buildings or 27 apartment complexes per node. However, the PV

generation for those nodes was moderate, ranging from 300 to 800 % of peak load in the net-zero PV sizing scenario. On the other hand, nodes 3, 6, 11, 12, and 13 were lightly loaded with only three medium office buildings or nine apartment complexes. Most of the light-loaded nodes constituted moderate amounts of distributed generation, except node 12 that showed high distributed generation up to 1,000 % of peak load in the net-zero PV sizing scenario. Smart inverter actuation range, defined as reactive power output in var, was scaled with a typical 30 % maximal output of the PV inverter. The smart inverters used allowed the maximization of DER installations while keeping power grid parameters, e.g., voltage and loading, within acceptable range. However, note that the MPC controller explored in this study did not include a power system model nor smart inverter actuation, and therefore a mismatch between integrated MPC and the simulation environment is present. Line types were allocated in a uniform fashion where transport lines, shown as bold, were 120 mm^2 Aluminium (Al) conductor and all others were 25 mm^2 Al. Lengths were taken from the original IEEE13 network and are marked as overlay in Figure 2, in meter. It can be seen that nodes 9, 11, 12, and 13 have the longest distances to the grid interconnection, i.e., node 1, and therefore the weakest electric interconnections.

Inequities in the system were considered bi-fold. First, the loading scenario chosen for this study inherently contains inequity by its stochastic allocation of load, generation, and battery storage. This limitation of generation or battery storage per node can be interpreted as limited roof space for PV or less available capital in disadvantaged communities. Second, each node of the electric distribution network is connected through a multitude of power lines which limits how many DERs can be installed. This results in inequity to grid reserves based on geographic location. Inequities are proposed to be mitigated by sharing community resources which leads to greater benefit for the whole community. For example, integrated control may share one site's large battery with another site where the total cost is reduced further than each site's individual cost, while maximizing resource utilization.

Simulations were carried out at Lawrence Berkeley National Laboratory's Lawrencium high performance computing facility using four LR6 nodes with Intel Xeon Gold 6130 processor with 16 cores, 2.1 GHz each, and 128 GB of memory.

Results

The following section shows highlighted results from the 3,200 simulations conducted, which included the two control strategies of integrated and individual control, two PV sizing scenarios of peak and net-zero, each with and without smart inverters, 16 weather clusters, and parametric grid of 25 battery sizes. Three-dimensional response surface plots were generated by grouping commercial and residential customers across the feeder. While this method partially obstructs inequities between same customer types, it helps visualize optimal battery patterns across the distinct commercial and residential customer types. Figure 3 shows the optimal response surfaces for two of the sixteen significant days.

The four columns correspond to the scenarios of PV sizing with or without smart inverters being present. The x-axis shows the aggregated commercial battery capacity and the y-axis shows the aggregated residential battery capacity. The battery capacity is defined as discharge duration for the peak building demand, in hours. For example, if two customers would have peak demands of 200 and 300 kW and the battery capacity is set to 2 hours, then the combined batteries from both sites would be capable of 500 kW discharge for 2 hours which is 1 MWh capacity. The z-axis shows the benefit of integration, in %, defined by the time-of-use electricity cost savings between individual and integrated control. The first subplot in the upper row shows the response surface for peak PV sizing scenario without smart inverters for April 26. The benefit of integration varies between 0.3 and 7.1 %. Greater benefit tends to be achieved when lager differences between commercial and residential battery sizes exist, e.g., when commercial battery size is close to 0 and residential battery size is 4 hours. The same results are apparent for the next subplot in the first row, showing peak PV sizing scenario with smart inverters. The lack of differences indicates that even though smart inverters are present, the sizing of PV for peak demand does not cause large stress on the power grid and limited actuation of smart inverters. When analyzing the third subplot in the first row showing the net-zero PV sizing scenario without smart inverters, the response surface for benefit of integration changes and largest benefit is now given when both residential and commercial batteries are at their maximum size, and lowest benefits are apparent when differences between the batteries are largest. While optimally sized batteries can provide benefits of up to 28.3 %, the benefits can also drastically decline down to -16.0 % when poorly sized. The addition of smart inverters shows minor differences when battery capacities

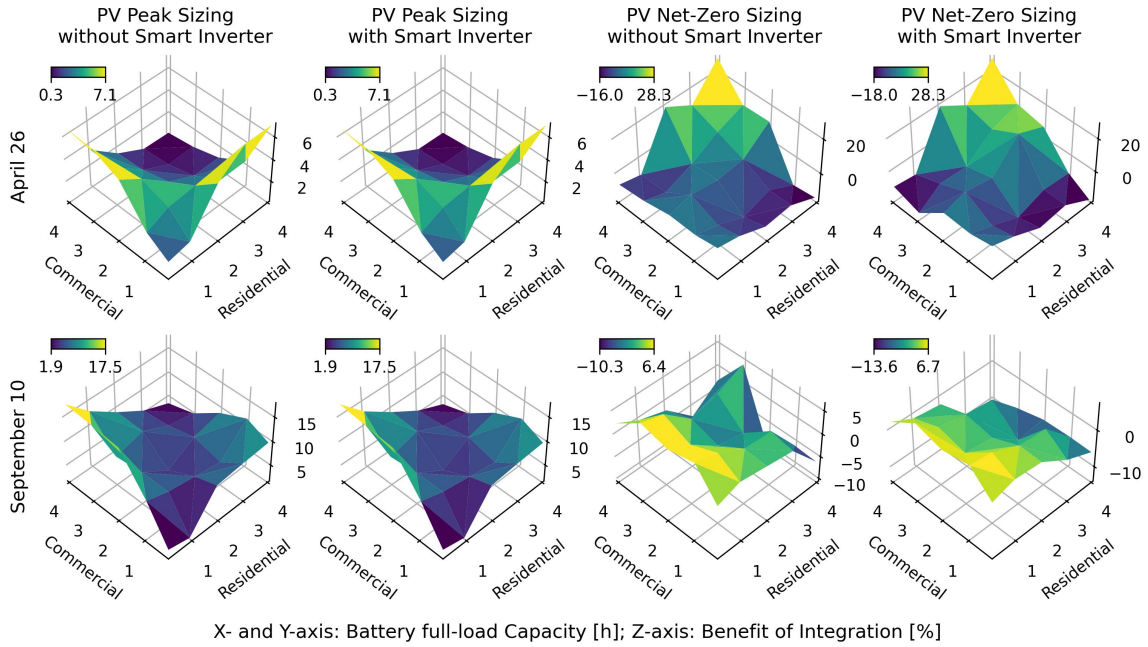

Figure 3: Example Response Surfaces for Benefit of Integration through Parametric Battery Sizes of Aggregated Commercial and Residential Sites for Four Scenarios (columns) and Two Days (rows).

are in the 2 hours range. The results for another day, September 10, in the second row of Figure 3 for the peak PV sizing scenarios show similar trends as the April 26 ones, but with higher potential savings between 1.9 to 17.5 %. This can likely be attributed to the TOU tariff which has steeper price differences between the demand periods in the summer season. The net-zero PV sizing scenarios on the other hand show optimal regions only when residential batteries are small. The scenario without smart inverters shows savings between -10.3 to 6.4 %. The scenario with smart inverters shows large differences in the region when both commercial and residential batteries are large, but otherwise matches the trends of the scenario without smart inverters. Savings range from -13.6 to 6.7 %.

The Table 1 shows the corresponding smart inverter actuation for a subset of the April 26 battery parameters shown in Figure 3. The columns include the PV sizing scenario, commercial and residential battery size, in hours, the active power curtailment statistics, in %, and reactive power injection statistics, in %. The first five samples show peak PV sizing. It can be seen that no active power curtailment is applied and reactive power control ranges between 0 to 64 %. All of the 12 load-bearing nodes provide some degree of reactive power control. On the other hand, the net-zero PV sizing scenario shows

Table 1: Samples of Inverter Actuation on April 26.

PV	Com/Res Size [h]	Curtail [%] min	Curtail [%] mean	Curtail [%] max	Reactive [%] min	Reactive [%] mean	Reactive [%] max
peak	4/4	0	0	0	0	31	64
peak	1/1	0	0	0	0	28	58
peak	2/1	0	0	0	0	29	60
peak	3/1	0	0	0	1	29	60
peak	4/1	0	0	0	2	30	61
net-z	4/4	0	0	4	0	7	98
net-z	1/3	0	0	22	0	15	100
net-z	4/1	0	0	23	0	13	100
net-z	0/3	0	0	30	0	17	100
net-z	0/2	0	0	32	0	20	100

significant amount of active power curtailment for most cases, except when both, commercial and residential batteries are maximally sized. Four of the 12 load-bearing nodes saturate the reactive power control and need to switch to active power curtailment with up to 32 % actuation. Figure 4 illustrates this scenario by providing spatial smart inverter actuation to highlight the associated inequity due to electric power grid constraints.

The Figure 4 shows a snapshot of the IEEE13 electric grid model at high PV generation time and 0/2 battery

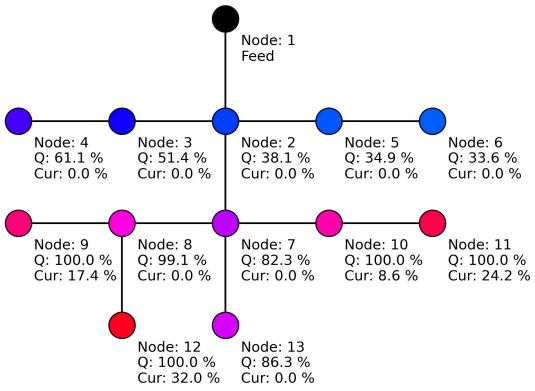

Figure 4: Example Smart Inverter Reactive Power (Q) and Active Power Curtailment (Cur) Actuation for 0 h Commercial and 2 h Residential Batteries on April 26.

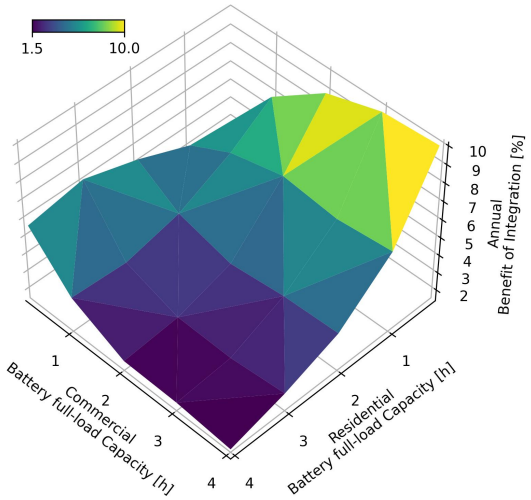

Figure 5: Annual Benefit of Integration for Peak PV Sizing.

ratio between commercial and residential, introduced in the last row of Table 1. The first node, in black, provides the interconnection with the larger power grid and feeds the radial distribution of customers. The color of the remaining nodes illustrates the total actuation of the respective smart inverter. Nodes in blue show moderate actuation whereas nodes in red show heavy actuation with active power curtailment. The large generation of PV and associated power exchange between nodes and the larger power grid leads voltages to raise. Customers at grid edges, e.g., nodes 9, 11, and 12, experience inequity since they are limited in the amount of power they can feed-in and must curtail active power by 17.4, 24.2, and 32.0 % respectively.

The Figure 5 shows the combination of the 16 weather clusters, weighted by the number of days within each cluster, to project annual cost savings for the peak PV sizing scenario. It shows an optimum when residential batteries are small and commercial batteries are moderate to large. The benefit of integration through electricity cost savings ranges from 1.5 to 10.0 % for the peak PV scenario, with seasonal minimum of -10.9 % and maximum of 23.5 %. The results for the net-zero PV scenario range from -10.1 to 0.9 % annually, with seasonal minimum of -42.8 % and maximum of 28.3 %.

Discussion

This work demonstrated how inequities can arise and the resulting non-linearity in benefit of integration for parametric battery sizes. Space and economic inequities were incorporated with the stochastic allocation of PV sizes across customers of the IEEE13 electric power grid model. The resulting imbalance in generation along customers lead to time-of-use electricity cost savings when systems are integrated. However, the inclusion of the electric power grid and its constraints lead to additional inequities based on the spatial distribution of customers. Those located at the end of the distribution system where electrical interconnections are typically the weakest experienced more smart inverter actuation including PV active power curtailment. This is exemplified for the net-zero PV penetration scenario, illustrated in Figure 4, where nodes 9, 11, and 12 experienced heavy smart inverter actuation, including active power curtailment up to 32 %. The response surfaces shown in Figure 3 support this finding: significant changes are observed between moderate PV generation scenario, i.e., peak PV sizing, and high PV generation scenario, i.e., net-zero PV sizing. Future asset allocation and control systems will need to provide flexibility to adjust to such changing circumstances to provide sustainable benefits through integrated energy systems. As illustrated in Figure 5, the electricity cost savings for the peak PV sizing scenario range up to 10.0 % on an annual basis and up to 23.5 % for seasonal periods. Greater annual benefit of integration tends to be achieved when residential batteries are small and commercial batteries are moderate to large. This indicates that it is more beneficial for commercial sites to support residential sites than vice versa. For the net-zero PV sizing scenario, the benefits of integration are generally lower which can be attributed to the MPC controller's lack of power grid and smart inverter mod-

els. Future versions might capture those dynamics and could lead to greater savings.

This study seeks to identify the technical potential of integrated energy systems and used MPC as exemplary controller. Here, the MPC-internal model and the underlying models of the simulation environment were artificially matched, with exclusion of the electric power grid in the MPC controller. Further research will be necessary to explore economic and market potentials. Key challenges for any controller will be the accurate forecasting of demand and renewable generation, as well as identifying system-internal dynamics, including battery efficiency and thermal mass in a building. Therefore, achievable cost savings in real installations will likely be less than shown in this study. Another simplification in this study was the application of TOU electricity cost as proxy for grid greenhouse gas emissions. While TOU electricity price schedules are loosely coupled to emissions, by the fact that conventional power plant's major operational cost is fuel which is converted to emissions, real-time grid emissions vary, e.g., due to the availability of renewable generation. Further work is needed to include bulk power system models to accurately account for generation dispatch and associated real-time emissions.

Another challenge concerns the mathematical and computational tools needed to discover economically feasible, zero-carbon, grid-level energy solutions from across the wide range of energy systems. For instance, the relatively confined simulations for only 12 individually-computed sites in this study took about 5 minutes each for a single battery size over a 24 hour period. Current methods do not allow for more than a few hundred individual customers, which limits the benefit IES could provide. The slow simulation time is also problematic as many applications of IES require annual or multi-year horizons to build and operate IES. Changing the horizon to one year would increase the simulation time of a single run to about 30 hours. In contrast, state of the art machine learning methods, such as reinforcement learning, require thousands of sequential iterations to discover optimal solutions. Therefore, scientific advancements in computational methods and dimension reduction are needed that can provide a clear analytical foundation to link functions of the electrical grid to near-real-time consumer use, and the vast opportunities provided by energy storage. This also includes advancements to optimize and ensure the security and reliability of this growing ecosystem. Those advancements are needed in the next few years to enable the transformation of infrastructure to realize the full potential of real-time energy controls that balance risk-aversion and risk-taking decisions for a future integrated energy infrastructure.

Conclusion

Integrated control of community energy systems poses a tremendous potential to lead the way to an economically feasible decarbonized future. The illustrated response surfaces for battery sizing highlight the nonlinear solution space and challenges when energy is exchanged across the community. Adequate sizing is crucial to maximize monetary and non-monetary benefits. This is especially true when including equity, distributed energy resources, building demand response control, and the electric power system. Further development of computational tools, regulatory guidelines, and customer acceptance will be necessary to successfully roll out community energy systems.

Acknowledgment

This work was supported by the Assistant Secretary for Energy Efficiency and Renewable Energy, Building Technologies Office of the U.S. Department of Energy under Contract No. DE-AC02-05CH11231.

References

Baker, Erin, Anna P Goldstein, and Inês ML Azevedo. 2021. "A perspective on equity implications of net zero energy systems." *Energy and Climate Change* 2:100047.

Bakhtavar, Ezzeddin, Tharindu Prabatha, Hirushie Karunathilake, Rehan Sadiq, and Kasun Hewage. 2020. "Assessment of renewable energy-based strategies for net-zero energy communities: A planning model using multi-objective goal programming." *Journal of Cleaner Production* 272:122886.

Brockman, Greg, Vicki Cheung, Ludwig Pettersson, Jonas Schneider, John Schulman, Jie Tang, and Wojciech Zaremba. 2016. "Openai gym." *arXiv preprint arXiv:1606.01540*.

Gehbauer, Christoph, Joscha Mueller, Tucker Swenson, and Evangelos Vrettos. 2020. "Photovoltaic and Behind-the-Meter Battery Storage: Advanced Smart Inverter Controls and Field Demonstration." *California Energy Comission*, no. CEC-500-2020-019.

Gehbauer, Christoph, Andreas Rippl, and Eleanor Lee. 2021. "Advanced Control of Dynamic Facades and HVAC with Reinforcement Learning based on Standardized Co-simulation." *Proceedings of the Building Simulation Conference 2021, in Bruges*.

Mendes, Gonçalo, Christos Ioakimidis, and Paulo Ferrão. 2011. "On the planning and analysis of Integrated Community Energy Systems: A review and survey of available tools." *Renewable and Sustainable Energy Reviews* 15 (9): 4836–4854.

Modelica, Association. 2022. The Functional Mock-up Interface. https://fmi-standard.org/. Accessed: 1/21/2022.

Neukomm, Monica, Valerie Nubbe, and Robert Fares. 2019. "Grid-interactive efficient buildings technical report series: Overview of research challenges and gaps." *U.S. Department of Energy - Office of Energy Efficiency and Renewable Energy*.

Nouidui, TS, DM Lorenzetti, and M Wetter. 2013. EnergyPlusToFMU. https://github.com/lbl-srg/EnergyPlusToFMU. Accessed: 1/21/2022.

Shandiz, Saeid Charani, Behzad Rismanchi, and Greg Foliente. 2021. "Energy master planning for net-zero emission communities: State of the art and research challenges." *Renewable and Sustainable Energy Reviews* 137:110600.

Vezzoli, Carlo, Fabrizio Ceschin, Lilac Osanjo, Mugendi K M'Rithaa, Richie Moalosi, Venny Nakazibwe, and Jan Carel Diehl. 2018. "Distributed/decentralised renewable energy systems." In *Designing Sustainable Energy for All*, 23–39. Springer.

Wetter, Michael, Wangda Zuo, Thierry S Nouidui, and Xiufeng Pang. 2014. "Modelica buildings library." *Journal of Building Performance Simulation* 7 (4): 253–270.